

Rapid Communications

Rapid Communications are intended for the accelerated publication of important new results and are therefore given priority treatment both in the editorial office and in production. A Rapid Communication in Physical Review B should be no longer than 4 printed pages and must be accompanied by an abstract. Page proofs are sent to authors.

Perpendicular transport in $a\text{-Si:H}/a\text{-SiN}_x\text{:H}$ single- and double-barrier structures

C. J. Arsenault, M. Meunier, M. Beaudoin, and B. Movaghar

*Groupe des Couches Minces and Département de Génie Physique, Ecole Polytechnique de Montréal,
Case Postale 6079, Succursale A, Montréal, Québec, Canada H3C 3A7*

(Received 8 April 1991; revised manuscript received 12 July 1991)

Current bumps in the current-voltage characteristics of amorphous semiconductor double-barrier structures have previously been associated with a resonant-tunneling process through quantized levels in the well region of the structure. We investigate the perpendicular transport through single- (SB) and double-barrier (DB) structures of hydrogenated amorphous silicon ($a\text{-Si:H}$) and hydrogenated amorphous silicon nitride ($a\text{-SiN}_x\text{:H}$) grown by glow discharge. The current-voltage characteristics of these structures are studied at 295 and 77 K. Current bumps are observed in the I - V characteristics of both SB and DB structures, which suggests a different transport mechanism than previously proposed. We propose that the first current bump is simply a transition from a low-field (space-charge-limited) transport mechanism to a high-field (multiple-hopping) transport mechanism. The additional bumps are associated with the energy dependence of the density of localized states in the $a\text{-SiN}_x\text{:H}$ and $a\text{-Si:H}$.

The optical and electrical properties of multilayered structures of amorphous semiconductors have been studied extensively by many groups since they were first proposed by Abeles and Tiedje.¹ Work on these layered amorphous semiconductors has concentrated mostly on their fundamental properties which appear to be similar to those of crystalline superlattices. Crystalline multilayer structures are known to exhibit many interesting properties associated with the quantum confinement of electrons and holes in the well region of these layered structures.

For amorphous semiconductor multilayers, one would expect quantum confinement to occur when the well width, d , is smaller than the *inelastic* scattering length, ℓ_i . However, all theoretical calculations^{2,3} on amorphous semiconductor multilayers do not use ℓ_i as the important length scale but rather compare the *elastic* scattering length (ℓ_e) to d . By treating the disorder as a random potential with zero correlation length, Raikh, Baranovskii, and Shklovskii² find that quantum confinement effects should occur when $d < 2\ell_e$. Tsu³ solved a damped one-dimensional wave equation and showed that quantum confinement effects would still be observable in well layers of 40 Å, even for an ℓ_e of only 4.5 Å. However, the criterion established in Ref. 2 would limit quantum size effects to well layers less than 9 Å. This discrepancy between theoretical models suggests that quantum confinement in amorphous semiconductor multilayers is still not completely understood.

Recent femtosecond spectroscopic studies^{4,5} have shown that electrons in extended states of the conduction band can be trapped by the band-tail states within a few hundred femtoseconds. Using this technique, Grahn *et*

*al.*⁶ have shown that the transport in the well layer ($d > 39$ Å) of $a\text{-Si:H}/a\text{-SiN}_x\text{:H}$ multilayers is dispersive. The temperature dependence of the dispersion parameter indicates that the carrier transport is multiple trapping for $T > 150$ K, while at lower temperatures hopping down in energy is the predominant mechanism. These results suggest that the carriers in $a\text{-Si:H}/a\text{-SiN}_x\text{:H}$ multilayered structures undergo inelastic collisions after traveling a distance less than the well layer thickness. Furthermore, these collisions would destroy the phase coherence necessary for the observation of quantum confinement effects.

The blueshift of the optical absorption edge^{1,7} and the shift of the photoluminescence peak⁸ with reduction of the well layer thickness are commonly used as proof of the quantum confinement of the carriers in the well layer of amorphous semiconductor superlattices. The increase of the field-effect mobility of multilayer thin-film transistors⁹ and the increase of the parallel resistivity of superlattices^{1,8} have also been explained using quantum confinement effects. However, several authors¹⁰⁻¹² have also proposed interpretations of these effects which do not rely on the quantum confinement of the carriers in the well layer.

Miyazaki, Ihara, and Hirose¹³ have associated current bumps in the I - V characteristics of doped $a\text{-Si:H}/a\text{-SiN}_x\text{:H}$ double-barrier (DB) structures to a resonant-tunneling phenomena through quantized levels in their doped amorphous silicon ($a\text{-Si:H}$) well layer. Pereyra *et al.*¹⁴ have also shown that current bumps in $a\text{-Si:H}/a\text{-SiC}_x\text{:H}$ DB structures can be accentuated using fast voltage sweep rates (up to 10 V/s) during the acquisition of the I - V curve. Carreño *et al.*¹⁵ later showed that similar

current bumps were observed in $a\text{-Si:H}/a\text{-SiC}_x\text{:H}$ single-barrier (SB) structures and structures with rectifying contacts. The dependence of the I - V characteristics of their SB and DB structures on the sweep rate was explained by a capacitive effect.

In this paper, we study the perpendicular-transport properties of undoped amorphous silicon ($a\text{-Si:H}$)/amorphous silicon nitride ($a\text{-SiN}_x\text{:H}$) DB structures. We chose not to dope the well layer since research on crystalline DB structures^{16,17} has shown that the presence of dopants in the well layer decreases significantly the scattering length of the electron and reduces considerably any resonant-tunneling effect. Furthermore, the mobility of doped $a\text{-Si:H}$ decreases with dopant concentration¹⁸ indicating an increase in electron scattering and a reduction of the scattering length. We show that the steady-state current bumps observed in both SB and DB structures can be explained by a trap-assisted tunneling process. This transport phenomena is very sensitive to the density of localized states in the barrier region and to the density of interface states between the barrier and well regions.

Figure 1 shows the SB and DB structures that were grown on heavily doped crystalline silicon ($c\text{-Si}$) substrates in a capacitively coupled rf glow discharge system. The n^+ -type $c\text{-Si}$ acted as the injecting contact to the SB and DB structures. Pure SiH_4 was used during the growth of the undoped $a\text{-Si:H}$ layer, while a gas mixture of NH_3/SiH_4 (10:1) was used for the $a\text{-SiN}_x\text{:H}$ layer. An 8% PH_3 in SiH_4 mixture was used for the heavily doped $a\text{-Si:H}$ top layer which acted as the collecting contact to the structures. The substrate temperature, rf power, and total pressure were held at 300°C , 10 W, and 200 mTorr, respectively. The glow discharge system and gas lines were evacuated quickly and purged for 50 min after each nitride layer in order to minimize any contamination of the undoped $a\text{-Si:H}$ layer. The base pressure after the

purge was $\sim 3 \times 10^{-6}$ Torr. The layer thicknesses for the SB and DB structures are indicated in Fig. 1. These thicknesses were estimated using the growth rate calculated from thicker bulk samples. The dark resistivities of these thick ($\sim 0.3 \mu\text{m}$) bulk samples were approximately 10^4 , 10^{15} , and $10^9 \Omega \text{ cm}$ for n^+ -type $a\text{-Si:H}$, $a\text{-SiN}_x\text{:H}$, and $a\text{-Si:H}$, respectively, which indicate the good quality of our layers.

The deposition of metal contacts and the mesa definition were performed in a clean-room environment (class 1000). Samples were dipped in diluted HF (1:10) and rinsed in DI H_2O immediately prior to metallization. Titanium (500 Å thick) was used as contact material to the n^+ -type $a\text{-Si:H}$ layer since it has a much lower barrier height ($\sim 0.3 \text{ eV}$) than Al ($\sim 1.0 \text{ eV}$).¹⁹ Without breaking the vacuum, a top layer of 1000 Å of gold was evaporated to prevent oxidation of the Ti contact. The Au/Ti contact was used as mask during the dry etching of the mesa in a $\text{CF}_4 + \text{O}_2$ plasma ($[\text{O}_2]/[\text{CF}_4] \approx 0.04$). The diameter of the mesa was $610 \mu\text{m}$.

The properties of our $a\text{-SiN}_x\text{:H}/a\text{-Si:H}$ interface were previously studied using x-ray photoelectron spectroscopy (XPS).²⁰ We showed that the interface obtained between near stoichiometric $a\text{-SiN}_x\text{:H}$ ($x = 1.4$) and $a\text{-Si:H}$ was atomically abrupt since subnitride components constituted less than 1% of the interface bonds. The valence-band offset for this interface was also obtained by following an analysis of the XPS valence-band spectra similar to that proposed by Iqbal *et al.*²¹ The measured valence-band offset of 1.3 eV is consistent with values previously published for an $a\text{-Si:H}/a\text{-SiN}_x\text{:H}$ interface.^{21,22} From the band gap of the bulk materials, the conduction-band offset was estimated to be 2.0 eV. The mobility edge variation estimated from these measurements is also shown in Fig. 1.

The I - V characteristics of the SB and DB structures are shown in Fig. 2 for 295 and 77 K. The applied bias corresponds to a positive voltage to the Au/Ti top contact. The opposite polarity consistently showed lower currents and less structure in the I - V curves. For this polarity, the electrons are injected into the n^+ -type $a\text{-Si:H}$ via the Ti contact which acts as a poor reverse-biased Schottky barrier. We have verified that all measurements are unaffected by changes in voltage scanning speeds from 10 to 100 mV/s. As compared to the scan speeds used by Carreño *et al.*,¹⁵ these scan speeds correspond to the very low-frequency regime where capacitive effects are very small.

From Fig. 2, we see that the 295 K I - V curves of the SB and DB structures present no important features. The 77 K I - V curves show a rapid increase at low V ($V < 0.1$) and a more gradual rise for larger voltages which might suggest the presence of a bump in the I - V curve close to 0.1 V. Miyazaki, Ihara, and Hirose¹³ associated a similar bump at low applied voltages to a resonant-tunneling process through the first quantized level of the well layer. However, it is highly unlikely that this bump near 0.1 V in the I - V curves of our samples can be attributed to a resonant-tunneling process since it is seen in almost all I - V curves of both SB and DB structures. We propose that this bump can be explained by a transition from a low-

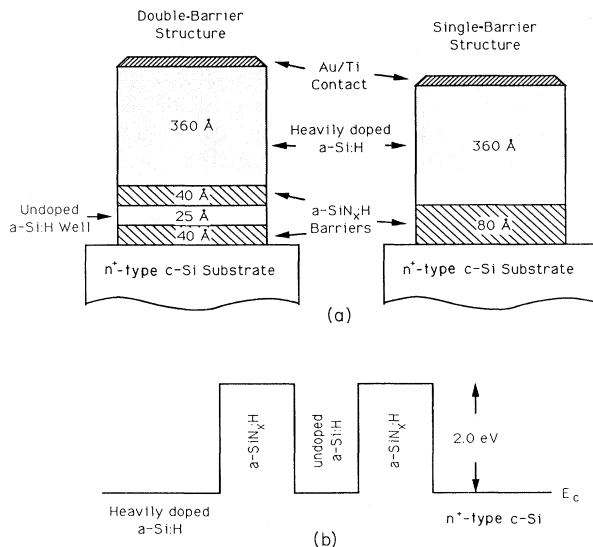


FIG. 1. Schematic illustration of the SB and DB structures along with the conduction-band mobility edge anticipated for the DB structure.

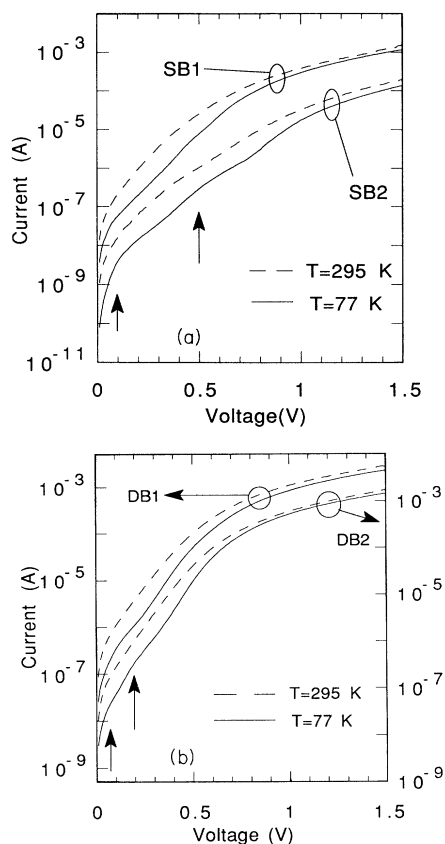


FIG. 2. Current-voltage characteristics of (a) two SB and (b) two DB structures measured at 295 K (dashed lines) and 77 K (solid lines). The arrows indicate the current bump positions.

field conduction mechanism (i.e., space-charge-limited current with $I \propto V^2$) to a high-field [i.e., high-field hopping with $I \propto \exp(\gamma F^\alpha)$, $\alpha \approx 0.5$] conduction mechanism.

The low-field transport mechanism in insulating material is known to exhibit ohmic behavior ($I \propto V$) at very low electric fields with an onset of space-charge-limited conduction at a critical field²³ of typically 10^3 – 10^4 V/cm. In comparison, the field across the thin insulating layer (~ 80 Å) of our SB structures is $\sim 10^5$ V/cm at an applied voltage of 0.1 V. Therefore, space-charge-limited currents should predominate at these low applied voltages.

As the field is increased, the transition probability between localized states is increased due to electric field heating of the localized electron. Furthermore, unoccupied states of higher energy are lowered by the field and can participate in the hopping conduction. Movaghar, Yelon, and Meunier²⁴ have shown that this kind of high-field transport leads to a field dependence of $\exp(\gamma F^\alpha)$ with $\alpha \sim 0.5$ for many different types of density of state distributions (e.g., constant, power law, exponential). As shown in Fig. 3, the fit using the V^2 dependence (space-charge-limited) and the $\exp(\gamma F^\alpha)$ dependence (high-field hopping transport) reproduces quite well the general behavior of the I - V characteristic of the SB structure presented in Fig. 2. The best fit was obtained using $\alpha = 0.45$.

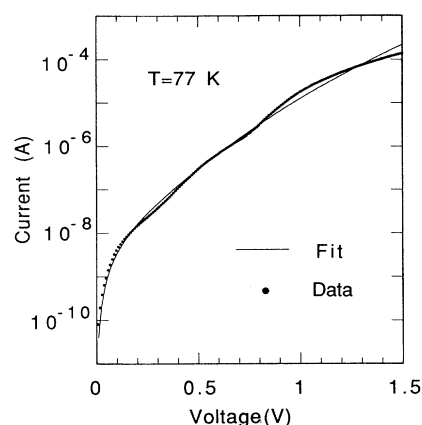


FIG. 3. Fit (solid line) of the SB1 I - V characteristic (points) at 77 K with a multiple-hopping model at high applied voltage and a space-charge-limited model at low applied voltage.

Since hopping conduction dominates at high fields, the fine detail in the high-field region of the I - V curve ($V > 0.2$ V) will be very sensitive to the density of the localized states in the barrier region as well as the density of interface states at the $a\text{-Si:H}/a\text{-SiN}_x\text{:H}$ interface. A strong energy dependence of these gap-state densities will produce structure in the I - V characteristics. Robertson and Powell²⁵ have shown that the Si dangling-bond distribution in $a\text{-SiN}_x\text{:H}$ lies about 2 eV below the mobility edge of the conduction band. The density of the dangling-bond states is quite large in $a\text{-SiN}_x\text{:H}$ (i.e., $\sim 10^{17}$ cm⁻³). In order to account for the current bump at 0.5 V in the SB structure of Fig. 2(a), the distribution of Si dangling-bond states should be located at about 0.25 eV above the Fermi level, which corresponds to ~ 1.75 eV below E_c of $a\text{-SiN}_x\text{:H}$ (see Fig. 1) and is consistent with the value published by Robertson and Powell.²⁵ In addition to the Si dangling-bond distribution within the $a\text{-SiN}_x\text{:H}$ barrier, the $a\text{-Si:H}/a\text{-SiN}_x\text{:H}$ interface states might also contribute to current bumps in the I - V characteristic.

The I - V curve of the DB structure [Fig. 2(b)] has current bumps at 0.07 and 0.2 V. Since current bumps are observed in both SB and DB structures, it is unlikely that these bumps result from a resonant-tunneling process. As for the SB structure, the first bump can be explained by the transition from a space-charge-limited conduction regime to a high-field hopping mechanism. The additional bump at 0.2 V is likely caused by the energy dependence in the density of localized states in the barrier regions (Si dangling-bond distribution) or in the distribution of interface states at both $a\text{-Si:H}/a\text{-SiN}_x\text{:H}$ interfaces.

For each structure (SB and DB) in Fig. 2, two mesas are presented which have been fabricated from the same sample and simultaneously submitted to the same processing steps. Yet, one mesa gives a current about 10 times lower. This variation in the current from otherwise identical mesas was observed on several samples. The presence of microchannels of a small cross-sectional area (< 1 μm^2) could explain these large variations in the current.

Microchannels have been proposed by Arce, Ley, and Hundhausen²⁶ to explain the occurrence of random telegraphic noise in large area (0.25 mm^2) $a\text{-Si:H}/a\text{-SiN}_x\text{:H}$ DB structures. Since these microchannels carry large current densities, a fluctuation in the density of these microchannels along the surface of the sample could explain the large variations in current observed from otherwise identical mesas. Interestingly, Arce, Ley, and Hundhausen²⁶ also studied the I - V characteristics of their DB structures and did not observe any current bumps which could be associated to a quantum size effect.

In conclusion, we explain the current bumps in the I - V characteristics of SB and DB $a\text{-Si:H}/a\text{-SiN}_x\text{:H}$ structures with a combination of transport mechanisms which do not rely on quantum confinement within the $a\text{-Si:H}$ well layer of the DB structure. We propose that the first current bump is simply a transition from a low-field (space-

charge-limited) transport mechanism to a high-field (multiple-hopping) transport mechanism. Since hopping transport increases with the density of hopping sites (i.e., localized states), the additional bumps can be associated to the energy dependence of the density of localized states in the $a\text{-SiN}_x\text{:H}$ and to the interface state energy distribution. The $a\text{-SiN}_x\text{:H}$ layer is known to have a large Si dangling-bond distribution at $\sim 2.0 \text{ eV}$ below the conduction-band mobility edge which could explain the current bumps observed in the I - V characteristic.

The authors are grateful to R. Izquierdo for his help in the XPS valence-band spectra measurements. The authors also wish to thank the "Conseil de Recherche en Sciences Naturelles et Génie du Canada" and the "Fondation des diplômés de l'École Polytechnique" for their financial assistance.

-
- ¹B. Abeles and T. Tiedje, *Phys. Rev. Lett.* **51**, 2003 (1983).
²M. E. Raikh, S. D. Baranovskii, and B. I. Shklovskii, *Phys. Rev. B* **41**, 7701 (1990).
³R. Tsu, in *Tetrahedrally-Bonded Amorphous Semiconductors*, edited by David Adler and Hellmut Fritzsche (Plenum, New York, 1985), p. 433.
⁴P. M. Fauchet, D. Hulin, A. Migus, A. Antonetti, J. Kolodzey, and S. Wagner, *Phys. Rev. Lett.* **57**, 2438 (1986).
⁵A. Mouchid, D. Hulin, R. Vanderhaghen, W. L. Nighan, Jr., K. Gzara, and P. M. Fauchet, *Solid State Commun.* **74**, 1197 (1990).
⁶H. T. Grahn, Z. Vardeny, J. Tauc, and B. Abeles, *Phys. Rev. Lett.* **59**, 1144 (1987).
⁷B. Abeles and T. Tiedje, in *Semiconductors and Semimetals*, edited by Jacques I. Pankove (Academic, New York, 1984), Vol. 21C, p. 407.
⁸M. Hirose, S. Miyazaki, and N. Murayama, in *Tetrahedrally-Bonded Amorphous Semiconductors* (Ref. 3), p. 441.
⁹M. Tsukude, Y. Uchida, and M. Matsumura, *Jpn. J. Appl. Phys. Pt. 2* **26**, L111 (1987).
¹⁰R. W. Collins and C.-Y. Huang, *Phys. Rev. B* **34**, 2910 (1986).
¹¹C. Reita, L. Mariucci, and G. Fortunato, *Jpn. J. Appl. Phys. Pt. 1* **29**, 1634 (1990).
¹²T. Tiedje, B. Abeles, and B. G. Brooks, *Phys. Rev. Lett.* **54**, 2545 (1985).
¹³S. Miyazaki, Y. Ihara, and M. Hirose, *Phys. Rev. Lett.* **59**, 125 (1987).
¹⁴I. Pereyra, M. N. P. Carreño, R. K. Onmori, C. A. Sasaki, A. M. Andrade, and F. Alvarez, *J. Non-Cryst. Solids* **97 & 98**, 871 (1987).
¹⁵M. N. P. Carreño, I. Pereyra, A. Komazawa, and A. T. Arasaki, *J. Non-Cryst. Solids* **114**, 762 (1989).
¹⁶E. Wolak, K. L. Lear, P. M. Pitner, E. S. Hellman, B. G. Park, T. Weil, J. S. Harris, Jr., and D. Thomas, *Appl. Phys. Lett.* **53**, 201 (1988).
¹⁷T. C. L. G. Sollner, P. E. Tannenwald, D. D. Peck, and W. D. Goodhue, *Appl. Phys. Lett.* **45**, 1319 (1984).
¹⁸J. M. Marshall, R. A. Street, and M. J. Thompson, *Phys. Rev. B* **29**, 2331 (1984).
¹⁹J. Kanicki, B. A. Scott, K. Inushima, and M. H. Brodsky, *J. Non-Cryst. Solids* **77 & 78**, 789 (1985).
²⁰M. Beaudoin, C. J. Arsenaault, R. Izquierdo, and M. Meunier, *Appl. Phys. Lett.* **55**, 2640 (1989).
²¹A. Iqbal, W. B. Jackson, C. C. Tsai, J. W. Allen, and C. W. Bates, *J. Appl. Phys.* **61**, 2947 (1987).
²²L. Yang, B. Abeles, W. Eberhardt, H. Stasiewski, and D. Sondericker, *Phys. Rev. B* **39**, 3801 (1989).
²³M. A. Lampert and P. Mark, *Current Injection in Solids* (Academic, New York, 1970).
²⁴B. Movaghar, A. Yelon, and M. Meunier, *Chem. Phys.* **146**, 389 (1990).
²⁵J. Robertson and M. J. Powell, *Appl. Phys. Lett.* **44**, 415 (1984).
²⁶R. Arce, L. Ley, and M. Hundhausen, *J. Non-Cryst. Solids* **114**, 696 (1989).